Carbohydrate Polymers 106 (2014) 172–178

Contents lists available at ScienceDirect

Carbohydrate Polymers

journal homepage: www.elsevier.com/locate/carbpol

Dissolution of mechanically milled chitin in high temperature water

Taku Michael Aida[a,*], Kenji Oshima[a], Chihiro Abe[a], Ryoma Maruta[a], Masayuki Iguchi[a], Masaru Watanabe[b], Richard L. Smith Jr.[a,b]

[a] *Graduate School of Environmental Studies, Tohoku University, Sendai, Aramaki Aza Aoba 6-6-11, Aoba-ku, Sendai 980-8579, Japan*
[b] *Research Center of Supercritical Fluid Technology, Tohoku University, Aramaki Aza Aoba 6-6-11, Aoba-ku, Sendai 980-8579, Japan*

ARTICLE INFO

Article history:
Received 4 December 2013
Received in revised form 31 January 2014
Accepted 4 February 2014
Available online 12 February 2014

Keywords:
Chitin
High temperature water
Mechanical milling
Reaction mechanism

ABSTRACT

Chitin is high in crystallinity in its natural form and does not dissolve into high temperature water (HTW), which often leads to decomposition reactions such as hydrolysis, deacetylation and dehydration when hydrothermally processed. In this work, we investigated the reactions of mechanically milled chitin in HTW. Mechanical milling pretreatment combined with HTW treatment improved the liquefaction of chitin giving a maximum water soluble fraction of 80%, where the untreated chitin was 55%. The reaction mechanism of the milled and raw chitin in HTW was shown to be different. For milled chitin, the dissolution of chitin occurred during the heating period to supercritical water conditions (400 °C) at short reaction times (1 min). Extended reaction time (10 min) led to decomposition products and aromatic char formation. For raw chitin, the dissolution of chitin in HTW did not occur, due to its high crystallinity, so that liquefaction proceeded via decomposition reactions.

1. Introduction

Chitin, the (1–4)-2-acetamido-2-deoxy-β-D-glucan, is industrially produced from marine resources (Muzzarelli, 2012; Muzzarelli et al., 2012). High crystallinity of chitin is often observed due to extensive intra- and inter-molecular hydrogen bonding (Draget, Smidsrod, & Skjak-Braek, 2002; Pearson, Marchessault, & Liang, 1960). Chitin and chitosan activate the macrophages, and are mucoadhesive, antimicrobial, biodegradable and non-toxic; therefore they are widely used for the repair of wounded human tissues (Muzzarelli, 2009), drug delivery and cancer diagnosis (Jayakumar, Menon, Manzoor, Nair, & Tamura, 2010; Jayakumar, Prabaharan, Kumar, Nair, & Tamura, 2011). Future applications are suggested; however, processing chitin is difficult, due to its high crystallinity and low solubility to solvents (Pearson et al., 1960; Takai et al., 1992). Solvents such as dimethylacetamide with LiCl (Brine & Austin, 1975; Tsioptsias & Panayiotou, 2008; Weng & Wang, 2001), methanol saturated calcium chloride dehydrate (Tamura, Nagahama, & Tokura, 2006), methanesulfonic acid (Nishi, Noguchi, Tokura, & Shiota, 1979), hexafluoroisopropanol and hexafluoroacetone sesquihydrate (Capozza RC. Solution of poly-(N-acetyl-D-glucosamine), US Patent 3; Carpozza RC. Spinning and shaping poly-(N-acetyl-D-glucosamine), US Patent 3; Louvier-Hernandez, Luna-Barcenas, Thakur, & Gupta, 2005; Salinas-Hernandez et al., 2009) have been reported to dissolve chitin. However these solvents are toxic and the utilization is not preferable for medical applications.

High temperature water (HTW) is an environmental friendly solvent. Solvent properties such as dielectric constant, viscosity, and dissociation constant can be varied by changing the temperature and pressure of the HTW (Akiya & Savage, 2002; Savage, 1999). Therefore, HTW can take place of organic solvents and acid–base catalysts. Natural polymers such as cellulose and hemicellulose depolymerize and dissolve into HTW due to the high concentration of hydronium and hydroxyl ions compared to water at room temperature (Sasaki, Fang, Fukushima, Adschiri, & Arai, 2000). Reports of treating chitin with HTW have been reported (Quitain, Sato, Daimon, & Fujie, 2001; Sakanishi, Ikeyama, Sakaki, Shibata, & Miki, 1999; Sato, 2004). In HTW, the liquefaction of chitin is suppressed due to its high crystallinity and high temperatures over 300 °C are required (Sakanishi et al., 1999; Yoshida, Ehara, & Saka, 2004). Amorphous chitin, prepared by a concentrated base and acid, showed that the hydrolysis reaction occurred in a much higher rate compared to the original chitin in HTW at 180 °C (Sato, 2004). These results suggest that the reaction mechanism of chitin in HTW is dependent to the degree of crystallinity of the chitin.

The crystallinity of biopolymers can be reduced by mechanically milling (Takeda et al., 2009; Craeyveld, Delcour, & Courtin,

---

[*] Corresponding author. Tel.: +81 022 795 5864; fax: +81 022 795 5864.
E-mail address: aida@scf.che.tohoku.ac.jp (T.M. Aida).

http://dx.doi.org/10.1016/j.carbpol.2014.02.009
0144-8617/

2008; Van Craeyveld et al., 2009; Venkataraman & Narayanan, 1998). This technique does not require any organic nor inorganic chemical. Mechanically milling has been shown to reduce the crystallinity of polymers such as cellulose (Sasaki et al., 2000) and chitin (Nakagawa et al., 2011). Osada et al. (2012) and Osada, Miura, et al., (2013) reported that a combination of milling and HTW pretreatment enhanced the enzymic decomposition from 5% (untreated chitin) up to 93%. In that work, it was reported that the increased enzymic degradation rate was due to the increased hydrophilicity of the pretreated chitin. However, to our knowledge, the dissolution of milled chitin in high temperature water has not yet been reported. The objective of this work is to investigate the reactions of raw and milled chitin in high temperature water and elucidate the reactions mechanisms.

2. Experimental

2.1. Materials

Chitin was obtained from Sigma–Aldrich and was used as received. Water was purified with a water distillation apparatus (Yamato Co., model WG-220) having a conductivity of 5.5 μs m^{-1}. Formic acid (>99%, Wako chemicals), 5-hydroxymethylfurfural (5-HMF) (99%>, Sigma–Aldrich), acetic acid (99.7%>, Wako chemicals), glycolic acid (>98%, Tokyo Chemical Industry Co., Ltd., Saitama, Japan), and dihydroxyacetone dimer (96%, Tokyo Chemical Industry Co., Ltd., Saitama, Japan) were used as standards for the HPLC analysis.

Milling of chitin was conducted in the interest of understanding the effect of polymer structure especially crystallinity on the dissolution phenomena of chitin. Chitin samples were grinded using a planetary ball mill (Pulverisette-7, Fritsch). A brief procedure is as follows. First, chitin (1.0 g) samples and 24 grinding balls (10 mm diameter) were loaded into a pair of grinding bowls (45 cm^3) and sealed. Both the grinding balls and grinding bowls were made of zirconium oxide. A pair of the loaded and sealed grinding bowls was attached to a revolution disk that was rotated at 700 rpm for 15 min followed by a 15 min rest period and this was repeated for 7 intervals. After the grinding, the milled chitin was removed from the pots for characterization and hydrothermal treatment experiments. The proximate and ultimate analysis of the raw chitin and milled chitin is shown in Table S1.

2.2. Characterization of the raw chitin and milled chitin

Characterization of the raw and the milled chitin samples were conducted. A simplified scheme of the mechanical pretreatment and the characterization preformed on the samples are shown in Fig. S1. Morphologies of the samples were observed by a scanning electron microscope (SEM) (JOEL JSM-6390, JOEL, Japan). Prior to the observation by the SEM, samples were pretreated by carbon deposition to eliminate charging and improve contrast of the SEM images. X-ray diffraction analysis (RU-200A, RIGAKU, Japan) was conducted on the samples to evaluate the crystallinity using a method reported in previous literature (Minke & Blackwell, 1978; Schiffman, Stulga, & Schauer, 2009). The mean particle diameter of the raw and milled chitin samples was measured by laser diffraction analysis (MT3300EX, NIKKISO, Japan). Chemical structures of the samples were investigated by Fourier transform FT-IR analysis (FT/IR-230, JASCO, Japan). Specific surface area of the samples was analyzed by volumetric gas adsorption (BELSORP-mini, BEL Japan), where the data reported are a result of the averages and standard deviations of two separate measurements. The solubility of the raw and milled chitin in water at room temperature was evaluated by the following procedure. First, raw or milled samples (0.1 g) were mixed in distilled water (3.0 g) in a flask at 25 °C for 2 h. After this treatment, the mixture was filtered to obtain a solid and solution. The obtained solid was dried at 60 °C for 24 h under vacuum. The solubility of the samples was evaluated by the net weight between the initial sample and solid obtained after the drying. The obtained solution was analyzed by MALDI-TOFMS to understand the molecular weight of the dissolved compounds. Also, to understand the chemical structure of the dissolved compounds in the solution, this solution was freeze-dried and the obtained solid was analyzed by FTIR.

2.3. Procedure

2.3.1. Hydrothermal treatment of chitin

The hydrothermal treatment of chitin was conducted on both raw and milled chitin samples. The simplified scheme of the experimental procedure and analysis is shown in Fig. S2. First, chitin samples (0.1 g) and distilled water (3.0 g) were loaded into a stainless steel (SUS316) tube bomb reactor with an inner volume of 6.0 cm^3. Then the contents of the reactor were purged with Argon atmosphere for removal of oxygen and then sealed. The reaction was initiated by immersion of the reactor into a fluidized sand bath controlled at the reaction temperature. The reaction temperatures examined were 220 and 400 °C. After the required reaction time, the reactor was quickly quenched by transferring the reactor from the sand bath into a water bath at room temperature. The reaction time was defined as the time when the reactor was first placed into the fluidized sand bath until the reactor was quenched in the water bath. The time required for the reactor to reach the reaction temperature (400 °C) was 4 min, while the time for cooling to below 100 °C was 30 s. The reaction times examined in this work were 1, 10 and 20 min. After the reactor was cooled, the contents of the reactor was washed out with distilled water (60 g) and filtered with a 10 μm membrane filter. The obtained solid was dried in a vacuum oven at 60 °C for 24 h and weighed in a weighing vial after cooling to room temperature in a dry desiccator under N_2 atmosphere. This solid was defined as the product solid. The solid recovery (SR) of chitin after hydrothermal treatment was evaluated by the following equation:

$$\text{Solid recovery}\,(\%) = \left[1 - \frac{W_{\text{product solid}}\,(\text{g})}{W_{\text{chitin}}\,(\text{g})}\right] \times 100 \qquad (1)$$

where $W_{\text{product solid}}$ and W_{chitin} are the weight of the product solid and the weight of the loaded chitin sample of the experiment.

The total carbon concentration of the liquid product was analyzed by a TOC (Shimadzu, model TOC-5000A) and the water soluble fraction (WS) of chitin was evaluated by the following equation.

$$\text{Water soluble fraction of chitin}\,(\%) = \frac{W_{\text{C\_liquid}}\,(\text{g})}{W_{\text{C\_chitin}}\,(\text{g})} \qquad (2)$$

where $W_{\text{C\_liquid}}$ and $W_{\text{C\_chitin}}$ are the amount of carbon in the liquid evaluated from the TOC analysis and the amount of carbon calculated from the elemental analysis respectively.

The liquid product was stored at room temperature for 24 h. After storing the liquid product for 24 h, solid precipitation was observed. The solid precipitate was collected by decantation and dried at 60 °C under vacuum. This solid was defined as the solid precipitate. SEM observation and FTIR analysis were done on the obtained solid precipitate.

Identification and quantification of the compounds obtained in the liquid product were evaluated by high performance liquid chromatography (HPLC). The HPLC system was equipped with a RI detector (RI SE-61, SHODEX), two RSpak KC-811 columns (Showa Denko) and H_3PO_4 aqueous solution (5 mM) was used as mobile phase at a flow rate of 1.0 mL/min at 80 °C. The products

Table 1
Comparison between (a) raw chitin and (b) milled chitin as a function of crystallinity, specific surface area, mean volume diameter and solubility in water at 25 °C.

	Crystallinity (%)	Specific surface area (m^2/g)	Mean volume diameter (μm)	Solubility[a] (%)
(a) Raw chitin	95	3.8 ± 0.8	628	3
(b) Milled chitin	0	0.96 ± 0.01	98	35

[a] Solubility in water at 25 °C.

detected were quantified according to the calibration curve constructed previously by the respective standards. A representative HPLC chromatograph is shown in supplementary material (Fig. S3). The detected liquid products were acetic acid, 5-HMF, formic acid, dihydroxyacetone and glycolic acid. Product yields were calculated on a carbon yield basis.

3. Results

3.1. The effect of mechanical milling treatment on the chemical and physical structure of chitin

Fig. S4 gives the SEM observation of raw chitin and milled chitin. As shown in Fig. S4a, raw chitin has a fiber like morphology, where milled chitin (Fig. S4b) has flake-like structures. There was no significant difference between raw chitin and milled chitin in CHNO composition (Table S1). Fig. S5a and S5b show the FTIR spectra of the raw chitin and the milled chitin respectively. Typical peaks of α-chitin have been reported in the literature (Gow, Gooday, Russell, & Wilson, 1987) as 894, 951, 1028, 1072, 1113, 1156, 1202, 1259, 1310, 1377, 1415, 1556, 1625, 1658 cm^{-1}. Fig. S5a and S5b show that both raw chitin and milled chitin had the same peaks as α-chitin. The FTIR results and the elemental analysis results show that the milling treatment did not change the chemical functional groups of the chitin.

Table 1 shows a comparison between the raw chitin and the milled chitin as a function of crystallinity, specific surface area, mean volume diameter and solubility in water at 25 °C. The specific surface area of the raw chitin and the milled chitin was $3.8 \pm 0.8\ m^2/g$ and $0.96 \pm 0.01\ m^2/g$ respectively. The crystallinity decreased from 95% to 0% due to the milling of raw chitin. The mean volume diameter of the raw chitin and the milled chitin was 628 μm and 98 μm respectively. The lower specific surface area and smaller mean volume diameter, for the milled chitin compared to the raw chitin sample, may be due to the decrease of the porous structures during the mechanical pulverization.

Milling the chitin increased the solubility in water at 25 °C where it was 3% for raw chitin and 35% for the milled chitin. To understand the chemical structure of the dissolved compounds in the aqueous solution of the milled chitin, this solution was freeze-dried and the solids obtained were analyzed by FT-IR as shown in Fig. S5(c). As shown in Fig. S5(c) the FT-IR spectrums of the freeze-dried solution of the milled chitin gave identical peaks to both raw chitin and milled chitin. This indicates that the milled chitin dissolved into water retaining its chitin chemical structure. Fig. S6 shows the MALDI of the solution obtained from dissolving milled chitin in water at 25 °C. Fig. S6 shows that characteristic peaks appear one monomer (N-acetylglucosamine) distance apart from each other. This indicates the presence of chitin oligomers in the solution. These peaks were not detected by dissolving raw chitin into water at room temperature. Raw chitin was depolymerized into oligomer size chitin particles during the milling treatment. The reduction of the polymer chain length and the decrease in crystallinity are probably the reasons for the high solubility obtained for the milled chitin in water compared with the raw chitin. The results are evidence that milled chitin can be dissolved into an aqueous solution at room temperature. The SEM images of the solid obtained from the freeze-dried milled chitin aqueous solution gave a needle like structure very different from the fibrous structure of the raw chitin and the flake like structure of milled chitin (Fig. S4(c)). This indicates that chitin solutions can be processed into materials for the desired applications using only water.

3.2. Effect of mechanical milling of chitin on the reaction chemistry in HTW

In this section, data for the HTW treatment of both raw chitin and milled chitin will be presented. Data on water soluble fraction (WS), solid recovery (SR), liquid product yields, solid SEM observation and solid FTIR analysis will be introduced briefly for discussion of reaction mechanisms for milled and raw chitin.

3.2.1. Water soluble fraction (WS) and solid recovery (SR) of raw and milled chitin after HTW treatment

The water soluble fraction (WS) and solid recovery (SR) obtained from the HTW treatment of chitin and milled chitin are given in Table 2. At constant temperatures, the WS and SR between raw and milled chitin showed different dependence toward reaction time.

For raw chitin, the WS was 3% and the SR was 94% at 220 °C and 20 min (run #1). This indicates that the liquefaction of raw chitin was not significant at 220 °C, whereas for milled chitin, at 220 °C constant temperature, the WS increased with increasing reaction time giving a maximum of 41% at reaction time 20 min and the SR gradually decreased from 71% to 56% when increasing the reaction time from 1 to 20 min (run #5, 6, 7). This result indicates that the milled chitin has a higher reactivity toward HTW at 220 °C compared with the raw chitin.

At constant temperature 400 °C, for raw chitin, the WS increased with increasing reaction time up to 55% at 10 min and then decreased to 49% at 20 min reaction time, where the SR decreased as reaction times increased giving a minimum of 16% at reaction time 20 min (run #2, 3, 4). This indicates that higher reaction temperatures increase the liquefaction reactions of raw chitin in HTW. Also, at 400 °C, both WS and SR decreased when increasing the reaction time from 10 to 20 min (run #3, 4). This suggests that at 400 °C HTW conditions, gasification reactions took place. For milled chitin, at constant temperature 400 °C, the WS gave the maximum of yield of 73% at the shortest reaction time (1 min) and then decreased to a constant yield around 51% as the reaction time increased to 20 min, where the SR gave a sharp decrease to 27% at 1 min reaction time and gradually became constant (18%) when increasing reaction time to 20 min (run #8, 9, 10). In this experiment, 4 min is required for the contents of the reactor to achieve 400 °C reaction temperature and at 1 min reaction time, the temperature in the reactor is about 320 °C. This indicates that most of the liquefaction of the milled chitin is complete within the heating period of the experiment. The decrease in both WS and SR yields observed from 1 to 10 min reaction time indicates that gasification reactions took place during the HTW treatment of milled chitin at 400 °C.

Different trends of WS and SR toward reaction time at constant temperature conditions between the raw and milled chitin indicate that the liquefaction of these samples in HTW occurs by different mechanisms especially at high temperature conditions (400 °C). For this reason, further discussion will be focused on experiments conducted at 400 °C.

Table 2
Water soluble fraction and solid recovery yields obtained from hydrothermal treatment of (a) raw chitin and (b) milled chitin.

Starting material	Reaction conditions			Water soluble fraction (%)	Solid recovery (%)
	Run #	Temperature (°C)	Time (min)		
(a) Raw chitin	1	220[a]	20	3.1	93.5
	2		1	5.8	98.6
	3	400[b]	10	55.4	21.0
	4		20	49.3	15.8
(b) Milled chitin	5		1	30.1	70.9
	6	220[a]	10	39.0	61.3
	7		20	41.2	55.6
	8		1	73.4	26.7
	9	400[b]	10	48.4	17.0
	10		20	51.0	18.4

[a] Reactions conducted at 220 °C were at vapor pressure.
[b] Reactions conducted at 400 °C were at water density 0.5 g/cm^3.

3.2.2. Liquid product yields

Fig. S7 and Table 3 show the liquid product yields obtained from the hydrothermal treatment of raw chitin and milled chitin. The major product obtained from the hydrothermal treatment of chitin was acetic acid, 5-HMF and minor products were glycolic acid and formic acid. The production of these compounds from chitin treatment in HTW has also been reported previously in the literature (Yoshida et al., 2004). The existence of these compounds show that the decomposition of chitin occurred during the hydrothermal treatment.

Acetic acid is obtained from the deacetylation reaction of chitin or its component glycosamine (Draget et al., 2002). High temperatures and long reaction times gave higher acetic acid yields for both raw and milled chitin. This indicates that the deacetylation reaction of chitin proceeds with increasing temperature and reaction time. The acetic acid yields obtained at 400 °C and 20 min were similar between raw and milled chitin (run #4, 10). It is probable that the degree of the deacetylation for both raw chitin and milled chitin were similar under these conditions.

The substance 5-HMF is obtained from the hydrolysis of chitin to glycosamine followed by deacetylation and dehydration reactions (Jun, Shao, Ho, Koetter, & Lech, 2003). At 400 °C, 5-HMF yields decreased when increasing the reaction time from 1 to 10 min for both milled and raw chitin. This is evidence that 5-HMF was consumed during the HTW treatment. The presence of 5-HMF promotes the formation of carbonaceous solids or humins which has been reported in a number of reports treating 5-HMF or carbohydrates in hydrothermal systems (Falco, Baccile, & Titirici, 2011; Sevilla & Fuertes, 2009). The decrease in 5-HMF yield and the decrease in WS yield are probably due to polymerization reactions associated with 5-HMF.

The total yield of the products detected in the HPLC was higher for the milled chitin compared to the raw chitin at identical HTW conditions especially at 220 °C conditions (Fig. S7). This indicates that the milled chitin is more reactive than the raw chitin in HTW. At 400 °C and long reaction times (10 and 20 min) both raw chitin and milled chitin gave acetic acid as the only product, within measurable peaks in the present HPLC system, with a similar yield 19–25%. At 400 °C and short reaction time (1 min), the WS of raw chitin was 5.8% (5-HMF 2%), where milled chitin gave a higher WS of 73.4% and a variety of products such as 5-HMF (5.1%), acetic acid (6.2%), formic acid (0.5%) and glycolic acid (0.5%). These results indicate that the reaction of raw and milled chitin proceeds under different mechanisms in HTW. To understand the reaction mechanisms of raw and milled chitin in HTW, solids obtained before and after the HTW treatment will be analyzed by FT-IR and observed by SEM.

3.2.3. FT-IR and SEM observation of solid products and solid precipitate

FT-IR and SEM observation was conducted on solid products and solid precipitate obtained from the HTW treatment of raw and milled chitin at 400 °C and different reaction times. The solid product and precipitate product were obtained for all HTW conditions conducted at 400 °C, except for the experiment that was conducted from raw chitin at short reaction time (1 min),

Table 3
Liquid product yields obtained from hydrothermal treatment of (a) raw chitin and (b) milled chitin.

Starting material	Reaction conditions			Product yield (%)			
	Run #	Temperature (°C)	Time (min)	Acetic acid	5-HMF	Formic acid	Glycolic acid
(a) Raw chitin	1	220[a]	20	0.4	0.6	0	0
	2		1	0.2	0.5	0	0
	3	400[b]	10	19	0	0	0
	4		20	24	0	0	0
(b) Milled chitin	5		1	0.4	0	0.1	0
	6	220[a]	10	2.0	4.4	0.3	0
	7		20	5.0	5.2	0.5	0.1
	8		1	6.2	5.1	0.5	0.5
	9	400[b]	10	23	0	0	0
	10		20	25	0	0	0

[a] Reactions conducted at 220 °C were at vapor pressure.
[b] Reactions conducted at 400 °C were at water density 0.5 g/cm^3.

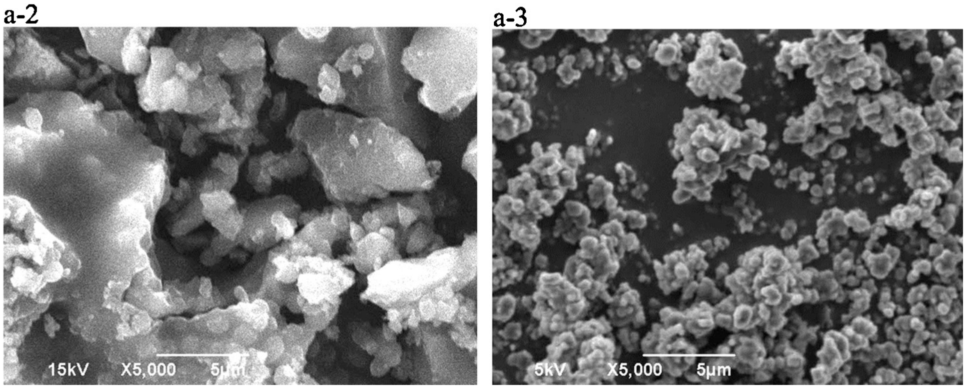

Fig. 1. SEM images of the (a-2) solid product and (a-3) solid precipitate obtained from the hydrothermal treatment of raw chitin conducted at 400 °C and reaction time 10 min.

where the precipitate solid could not be obtained probably due to low WS (5.8%) at this condition.

The SEM images of the solids obtained from the HTW treatment of raw chitin conducted at 400 °C and 10 min showed a smooth structure for solid product (Fig. 1a-2) and a structure of small particles aggregated together for the solid precipitate (Fig. 1a-3). These solids had different morphologies compared to the fibrous structure of the raw chitin (Fig. S4a). This indicates that the destruction of the chitin morphology occurred with the HTW treatment. Fig. 2 shows the FT-IR spectrum of raw chitin and the solids obtained after HTW treatment at 400 °C. The FT-IR spectrum of the raw chitin (Fig. 2a) and solid product (Fig. 2a-1) are similar. This indicates that the HTW treatment at 400 °C and 1 min reaction time did not change the chemical structure of the raw chitin. On the other hand, the solid product (Fig. 2a-2) and solid precipitate (Fig. 2a-3) gave very different FT-IR spectra from raw chitin (Fig. 2a) such as aromatic carbon carbon bond stretching absorbance at 1600 cm^{-1} (Marue, 1994) and peaks related to aromatic C—H out-of-plane

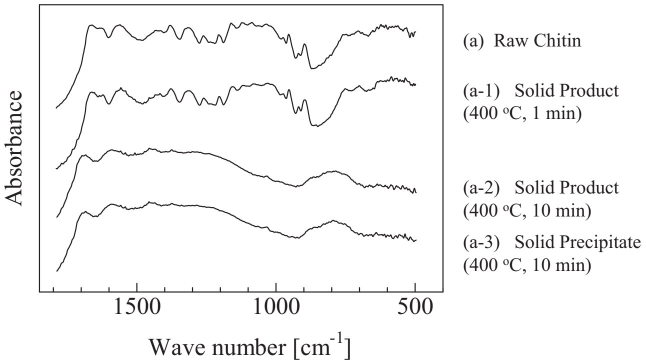

Fig. 2. FT-IR spectrum of (a) raw chitin and the (a-1 and a-2) solid product and (a-3) solid precipitate obtained from the hydrothermal treatment of raw chitin conducted at 400 °C, reaction time 1 and 10 min.

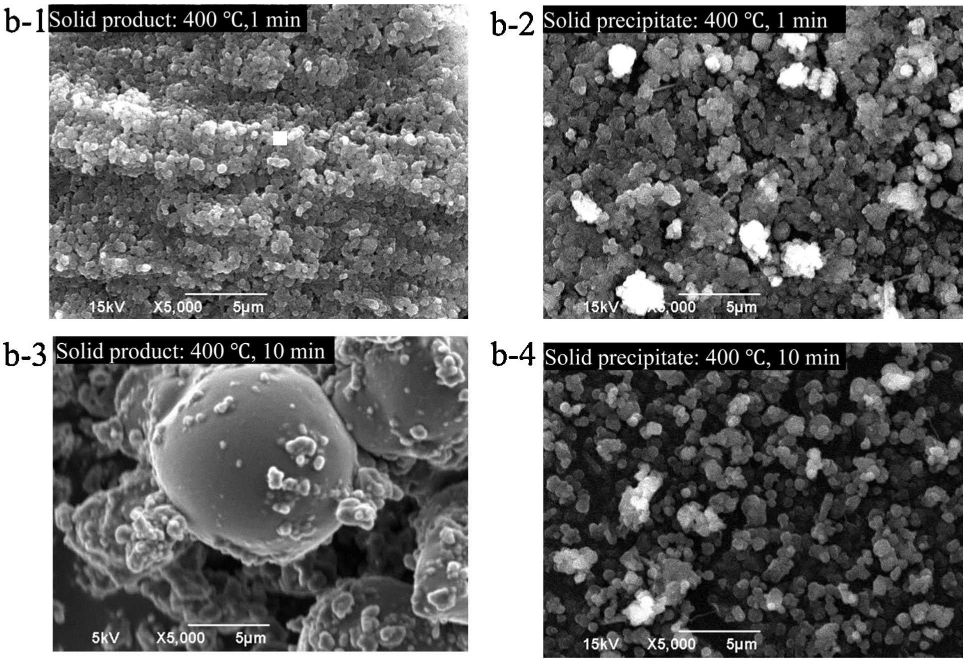

Fig. 3. SEM images of the (b-1 and b-3) solid product and (b-2 and b-4) solid precipitate obtained from the hydrothermal treatment of milled chitin conducted at 400 °C, reaction times 1 and 10 min.

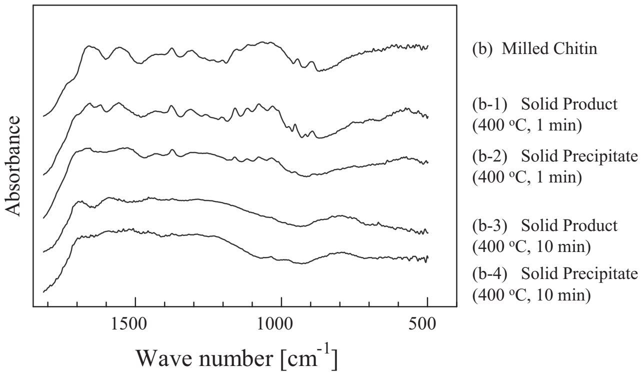

Fig. 4. FT-IR spectra of (b) milled chitin (b-1 and b-3) solid product and (b-2 and b-4) solid precipitate obtained from the hydrothermal treatment of milled chitin conducted at 400 °C, reaction time 1 and 10 min.

bending vibrations at 750–875 cm^{-1} (Lua & Yang, 2004). Based on this result and the results obtained from the liquid product analysis, it is probable that decomposition reactions (deacetylation, hydrolysis, dehydration) of chitin were promoted in HTW and then the carbonization reaction of 5-HMF occurred forming solids with aromatic structures (Falco et al., 2011; Sevilla & Fuertes, 2009).

Solids obtained from the HTW treatment of milled chitin differed between short (1 min) and long (10 min) reaction times. Figs. 3 and 4 show the SEM images and FT-IR spectrums of solid product (b-1 and b-3) and solid precipitate (b-2 and b-4) obtained from the HTW treatment of milled chitin at 400 °C and reaction times 1 and 10 min. At short HTW treatment times (1 min), solid product (Fig. 3b-1) and solid precipitate (Fig. 3b-2) had a fine powder like morphology. This was different compared to the flake like morphology observed for milled chitin in Fig. S4b. The FT-IR spectrums between the milled chitin (Fig. 4b) and solid product (Fig. 4b-1) and solid precipitate (Fig. 4b-2) did not show any significant difference. These results indicate for milled chitin, dissolution reactions mainly occurred in HTW at short reaction times (1 min).

However at long reaction times (10 min), the particle morphology of the solid product (Fig. 3b-3) show a bigger particle size compared to the powdery morphology observed in solid product (Fig. 3b-1). This indicates that solid forming reactions occurred when increasing the reaction time from 1 to 10 min. FT-IR spectrums of solid product (Fig. 4b-3) and solid precipitate (Fig. 4b-4) showed different compared to milled chitin (Fig. 4b), and very similar to the solid product (Fig. 2a-2) and solid precipitate (Fig. 2a-3). At long reaction times (10 min), it is probable that secondary reactions seen during the hydrothermal treatment of raw chitin also occurred for the milled chitin.

3.3. Reaction mechanism of chitin and milled chitin in HTW

Based on the findings, the reaction mechanism of chitin and milled chitin in high temperature water is different. A reaction schematic of raw chitin and milled chitin in HTW is given in Fig. 5. Raw chitin has a high crystallinity (95%) so that the bonds between the chitin chain are very strong and water can only access the surface. Therefore, at short reaction times of 1 min, dissolution of chitin and reactions such as hydrolysis are slow, and the product is unreacted chitin. However, at long reaction times of 10 and 20 min, the following occur in HTW: (1) hydrolysis reactions of chitin at the surface to form water soluble compounds, (2) decomposition of the chitin within the chitin polymer structure, (3) decomposition and polymerization of water soluble compounds. The resulting products are gas, acetic acid and a solid product with an aromatic chemical structure.

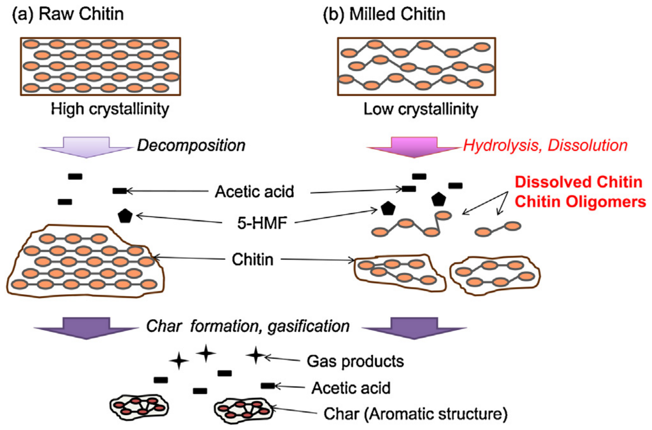

Fig. 5. Schematic of (a) raw chitin and (b) milled chitin reactions in high temperature water.

Milled chitin has a lower crystallinity compared to raw chitin. Therefore, in milled chitin, the number of physical cross-links is fewer than in raw chitin. At high temperatures, the mobility of the polymer with fewer cross-links would be greater. At high temperature conditions, water is able to diffuse within the chitin polymer and reactions between water and chitin such as hydrolysis and dissolution are fast compared to raw chitin. At short reaction times (1 min) hydrolysis reactions depolymerizing chitin occur readily within the chitin polymer, and dissolve low molecular weight chitin oligomers into solution. Secondary reactions of the water soluble chitin oligomers occur readily, and compounds such as acetic acid and 5-HMF are formed. The decomposition reactions of the unit monomer of chitin (N-acetyl-D-glucosamine) may have also occurred in high temperature water (Osada, Kikuta, et al., 2013). At long reaction times (10 and 20 min), secondary reactions of water soluble proceed such as gasification and polymerization of 5-HMF. Osada, Miura, et al., (2013) reported that the crystal size as well as the crystallinity of the chitin increased during the HTW treatment at 400 °C. This increase in crystallinity would suppress the dissolution of the chitin and may explain the similarity of the products obtained between the raw chitin and milled chitin at 400 °C and long reaction times (10 and 20 min). Increasing the reaction temperature will increase the dissolution of chitin only at short reaction times for milled chitin. Extending the reaction time will increase the secondary reactions of the dissolved chitin such as polymerization and gasification reactions.

4. Conclusions

Mechanical pretreatment combined with HTW treatment at high temperatures (400 °C) improves the liquefaction of chitin giving a maximum water soluble fraction of 73%, where the untreated chitin was 55% both at 400 °C conditions. For milled chitin, the dissolution occurs in high temperature water at short reaction times (1 min) and at long reaction times (10 and 20 min) decomposition products and aromatic chars form. For raw chitin, dissolution of chitin in high temperature water does not occur, due to high crystallinity, and mainly the liquefaction is via decomposition reactions.

Mechanical milling combined with high temperature water treatment is a promising method in processing chitin for future applications. Higher reaction temperatures, higher heating rates and shorter reaction times conducted in this study may enhance the liquefaction of milled chitin in HTW due to the suppression of secondary reactions such as gasification and char formation reactions. An investigation using a flow reactor that can achieve high temperatures (above 400 °C) and short reaction times (below 1 s) is in progress to check this assumption.

Acknowledgments

We would like to thank Dr. Junya Kano (Tohoku University Japan) for the mechanical pretreatment of chitin, Mr. Hiroaki Saito, Ms. Aya Haneda and Mr. Shunsuke Kayamori (Tohoku University, Japan) for the TEM analysis, Dr. Nagao (Tohoku University, Japan) for the XRD analysis and Dr. Atsushi Kobayashi and Mr. Naoki Yoshida (Tohoku University, Japan) for the MALDI-TOFMS analysis. Financial support from Global COE is gratefully acknowledged. We would also like to thank Mr. Haruo Ura (Hokkaido Research Organization, Japan) for the fruitful discussion during the research.

Appendix A. Supplementary data

Supplementary data associated with this article can be found, in the online version, at http://dx.doi.org/10.1016/j.carbpol.2014.02.009.

References

Akiya, N., & Savage, P. E. (2002). Roles of water for chemical reactions in high-temperature water. *Chemical Reviews*, *102*(8), 2725–2750.

Brine, C. J., & Austin, P. R. (1975). *Renatured chitin fibrils, films, and filaments. ACS Symposium Series* (vol. 18) Oxoford University press.

Capozza, R. C. (1976). Solution of poly-(N-acetyl-D-glucosamine). US Patent 3535.

Carpozza, R. C. (1976). Spinning and shaping poly-(N-acetyl-D-glucosamine). US Patent 3411.

Draget, K. I., Smidsrod, O., & Skjak-Braek, G. (2002). Biopolymers. In A. Steinbuchel (Ed.), *Polysaccharides II: Polysaccharides from eukaryotes* (pp. 481–557). Weinheim: Wiley-VCH Verlag GmbH.

Falco, C., Baccile, N., & Titirici, M. M. (2011). Morphological and structural differences between glucose, cellulose and lignocellulosic biomass derived hydrothermal carbons. *Green Chemistry*, *13*(11), 3273–3281.

Gow, N. A. R., Gooday, G. W., Russell, J. D., & Wilson, M. J. (1987). Infrared and X-ray-diffraction data on chitins of variable structure. *Carbohydrate Research*, *165*(1), 105–110.

Jayakumar, R., Menon, D., Manzoor, K., Nair, S. V., & Tamura, H. (2010). Biomedical applications of chitin and chitosan based nanomaterials—A short review. *Carbohydrate Polymers*, *82*(2), 227–232.

Jayakumar, R., Prabaharan, M., Kumar, P. T. S., Nair, S. V., & Tamura, H. (2011). Biomaterials based on chitin and chitosan in wound dressing applications. *Biotechnology Advances*, *29*(3), 322–337.

Jun, M., Shao, Y., Ho, C. T., Koetter, U., & Lech, S. (2003). Structural identification of nonvolatile dimerization products of glucosamine by gas chromatography–mass spectrometry, liquid chromatography–mass spectrometry, and nuclear magnetic resonance analysis. *Journal of Agricultural and Food Chemistry*, *51*(21), 6340–6346.

Louvier-Hernandez, J. F., Luna-Barcenas, G., Thakur, R., & Gupta, R. B. (2005). Formation of chitin nanofibers by supercritical antisolvent. *Journal of Biomedical Nanotechnology*, *1*(1), 109–114.

Lua, A. C., & Yang, T. (2004). Effect of activation temperature on the textural and chemical properties of potassium hydroxide activated carbon prepared from pistachio-nut shell. *Journal of Colloid and Interface Science*, *274*(2), 594–601.

Marue, T. (1994). FT-IR spectroscopic studies of major organic matter in carbonaceous chondrites using microscopic technique and comparison with terrestrial kerogen. In *NIPR symposium on Antarctic meteorites, Vol. 7* (pp. 262–274).

Minke, R., & Blackwell, J. (1978). Structure of alpha-chitin. *Journal of Molecular Biology*, *120*(2), 167–181.

Muzzarelli, R. A. A. (2009). Chitins and chitosans for the repair of wounded skin, nerve, cartilage and bone. *Carbohydrate Polymers*, *76*(2), 167–182.

Muzzarelli, R. A. A. (2012). Nanochitins and nanochitosans, paving the way to eco-friendly and energy-saving exploitation of marine resources. *Polymer Science: A Comprehensive Reference*, *10*, 153–164.

Muzzarelli, R. A. A., Boudrant, J., Meyer, D., Manno, N., DeMarchis, M., & Paoletti, M. G. (2012). Current views on fungal chitin/chitosan, human chitinases, food preservation, glucans, pectins and inulin: A tribute to Henri Braconnot, precursor of the carbohydrate polymers science, on the chitin bicentennial. *Carbohydrate Polymers*, *87*(2), 995–1012.

Nakagawa, Y. S., Oyama, Y., Kon, N., Nikaido, M., Tanno, K., Kogawa, J., et al. (2011). Development of innovative technologies to decrease the environmental burdens associated with using chitin as a biomass resource: Mechanochemical grinding and enzymatic degradation. *Carbohydrate Polymers*, *83*(4), 1843–1849.

Nishi, N., Noguchi, J., Tokura, S., & Shiota, H. (1979). Studies on chitin. 1. Acetylation of chitin. *Polymer Journal*, *11*(1), 27–32.

Osada, M., Kikuta, K., Yoshida, K., Totani, K., Ogata, M., & Usui, T. (2013). Non-catalytic synthesis of chromogen I and III from N-acetyl-D-glucosamine in high-temperature water. *Green Chemistry*, *15*(10), 2960–2966.

Osada, M., Miura, C., Nakagawa, Y. S., Kaihara, M., Nikaido, M., & Totani, K. (2012). Effect of sub- and supercritical water pretreatment on enzymatic degradation of chitin. *Carbohydrate Polymers*, *88*(1), 308–312.

Osada, M., Miura, C., Nakagawa, Y. S., Kaihara, M., Nikaido, M., & Totani, K. (2013). Effects of supercritical water and mechanochemical grinding treatments on physicochemical properties of chitin. *Carbohydrate Polymers*, *92*(2), 1573–1578.

Pearson, F. G., Marchessault, R. H., & Liang, C. Y. (1960). Infrared spectra of crystalline polysaccharides. 5. Chitin. *Journal of Polymer Science*, *43*(141), 101–116.

Quitain, A. T., Sato, N., Daimon, H., & Fujie, K. (2001). Production of valuable materials by hydrothermal treatment of shrimp shells. *Industrial & Engineering Chemistry Research*, *40*(25), 5885–5888.

Sakanishi, K., Ikeyama, N., Sakaki, T., Shibata, M., & Miki, T. (1999). Comparison of the hydrothermal decomposition reactivities of chitin and cellulose. *Industrial & Engineering Chemistry Research*, *38*(6), 2177–2181.

Salinas-Hernandez, R., Ruiz-Trevino, F. A., Ortiz-Estrada, C. H., Luna-Barcenas, G., Prokhorov, Y., Alvarado, J. F. J., et al. (2009). Chitin microstructure formation by rapid expansion techniques with supercritical carbon dioxide. *Industrial & Engineering Chemistry Research*, *48*(2), 769–778.

Sasaki, M., Fang, Z., Fukushima, Y., Adschiri, T., & Arai, K. (2000). Dissolution and hydrolysis of cellulose in subcritical and supercritical water. *Industrial & Engineering Chemistry Research*, *39*(8), 2883–2890.

Sato, K. (2004). Hydrothermal decomposition of chitin and chitosan. In S. Hirano (Ed.), *Development and technology of chitin and chitosan* (pp. 62–69). Tokyo: CMC-Publishing Co., Ltd.

Savage, P. E. (1999). Organic chemical reactions in supercritical water. *Chemical Reviews*, *99*(2), 603–621.

Schiffman, J. D., Stulga, L. A., & Schauer, C. L. (2009). Chitin and chitosan: Transformations due to the electrospinning process. *Polymer Engineering and Science*, *49*(10), 1918–1928.

Sevilla, M., & Fuertes, A. B. (2009). The production of carbon materials by hydrothermal carbonization of cellulose. *Carbon*, *47*(9), 2281–2289.

Takai, M., Shimizu, Y., Hayashi, J., Tokura, S., Ogawa, M., Kohriyama, T., et al. (1992). In W. E. A. Glasser (Ed.), *Structure–property relationship of alpha-chitin and beta-chitin*. Washington, DC: ACS Symposium Series.

Takeda, T., Nikaido, M., Totani, T., Obara, M., Nakano, Y., & Uchimiya, H. (2009). Evaluation of high intensive ball mill method for effective saccharification of plant cell wall materials. *Journal of Applied Glycoscience*, *56*, 71–76.

Tamura, H., Nagahama, H., & Tokura, S. (2006). Preparation of chitin hydrogel under mild conditions. *Cellulose*, *13*(4), 357–364.

Tsioptsias, C., & Panayiotou, C. (2008). Foaming of chitin hydrogels processed by supercritical carbon dioxide. *Journal of Supercritical Fluids*, *47*(2), 302–308.

Van Craeyveld, V., Delcour, J. A., & Courtin, C. M. (2008). Ball milling improves extractability and affects molecular properties of Psyllium (*Plantago ovata* Forsk) seed husk arabinoxylan. *Journal of Agricultural and Food Chemistry*, *56*(23), 11306–11311.

Van Craeyveld, V., Holopainen, U., Selinheimo, E., Poutanen, K., Delcour, J. A., & Courtin, C. M. (2009). Extensive dry ball milling of wheat and rye bran leads to in situ production of arabinoxylan oligosaccharides through nanoscale fragmentation. *Journal of Agricultural and Food Chemistry*, *57*(18), 8467–8473.

Venkataraman, K. S., & Narayanan, K. S. (1998). Energetics of collision between grinding media in ball mills and mechanochemical effects. *Powder Technology*, *96*(3), 190–201.

Weng, J., & Wang, M. (2001). Producing chitin scaffolds with controlled pore size and interconnectivity for tissue engineering. *Journal of Materials Science Letters*, *20*(15), 1401–1403.

Yoshida, K., Ehara, K., & Saka, S. (2004). In S. Hirano (Ed.), *Development and technology of chitin and chitosan* (pp. 51–69). Tokyo: CMC-Publishing Co., Ltd.